Structural Chemistry, Vol. 5, No. 1, 1994

Determination of Structure and Conformation in Solution of Syringotoxin, a Lipodepsipeptide from *Pseudomonas syringae* pv. *syringae* by 2D NMR and Molecular Dynamics

Alessandro Ballio,[1] Antonella Collina,[2] Alfredo Di Nola,[3] Cesare Manetti,[3] Maurizio Paci,[4,5] and Annalaura Segre[2]

Received August 31, 1992; accepted January 20, 1993

Strain B427 of *Pseudomonas syringae* pv. *syringae*, originally isolated from lemon, produces several bioactive lipodepsipeptides. The structure of Syringotoxin (ST) and Syringopeptins (SPs) has been investigated in these last years. This paper reports the 2D NMR data collected in the study of ST covalent structure. The study was performed in different solvents in order both to prevent aggregation and to completely characterize the side chains features. These include the presence of common and less common aminoacids, which compose the macrocyclic ring and fatty acid side-chain moieties of ST. The nature and position in the molecule of the residues involved in the lactonic ring closure of ST have been identified with certainty. The interpretation of NOE data obtained in acetonitrile/water solution was performed by molecular dynamics calculations in vacuo. This procedure has allowed determination of the nature and number of intramolecular hydrogen bonds and the predominant conformation of ST.

KEY WORDS: Syringotoxin, *Pseudomonas syringae*, lipodepsipeptides, 2D NMR, molecular mechanics.

INTRODUCTION

Syringotoxin (ST) is the name given to partially purified phytotoxic and fungicidal preparations obtained from phytopathogenic strains of *Pseudomonas syringae* pv. *syringae* isolated from citrus trees [1]. A preliminary study of ST structure yielded results favoring a peptide structure, since equimolar amounts of threonine, serine, glycine, ornithine, and an unidentified basic amino acid were formed on acid hydrolysis [2, 3].

Recent studies have demonstrated that these partially purified preparations contain more than one bioactive metabolite. In fact, HPLC of samples prepared from culture of strain B427 evidenced three main components, corresponding to a lipodepsinonapeptide for which the ST name has been retained [4] and two more hydrophobic lipodepsieicosipentapeptides, called syringopeptins SP-25A and SP-25B [5]. The biological activities of unfractionated mixtures are differently distributed between ST and SPs: pure ST exhibits high antifungal and moderate phytotoxic properties, and SP-25A is strongly phytotoxic and nearly devoid of antifungal activity [6]. The biological activity of SP-25B has not yet been investigated, but should not differ from that of SP-25A due to the nearly identical structure of the two compounds [5].

The elucidation of the covalent structure of ST has represented a necessary step in the study of the function and mode of action of this interesting metabolite [4, 7]. The assessment of its conformation has been taken into consideration in order to acquire further information useful for understanding the interaction of ST with specific components of the cell machinery and some of its physicochemical properties.

This paper reports in detail the 2D NMR data collected in the study of ST covalent structure [4], which

[1] Dipartimento di Scienze Biochimiche "A Rossi Fanelli," Universita' di Roma "La Sapienza," Roma, Italy.
[2] Istituto di Strutturistica Chimica, CNR, Montelibretti, Roma, Italy.
[3] Dipartimento di Chimica, Università di Roma "La Sapienza," Roma, Italy.
[4] Dipartimento di Scienze e Tecnologie Chimiche, Università "Tor Vergata," 00173 Roma, Italy.
[5] Correspondence should be directed to Maurizio Paci.

1040-0400/94/0200-0043$07.00/0

substantially agree with those reported [7], as well as the interpretation of Nuclear Overhauser effect (NOE) data obtained in acetonitrile/water solution by molecular dynamics calculations in vacuo; the latter has allowed us to determine the nature and number of intramolecular hydrogen bonds and the predominant conformation of ST.

RESULTS AND DISCUSSION

The use of different solvents in the NMR spectra allowed a complete individual assignment of the residues and the acquisition of all the sequential information. In fact, the usual methods for obtaining these results, such as the change in physicochemical parameters (i.e., temperature or pH), were not suitable in this case due to the limited stability of the sample and to the tendency to aggregate in water, giving a micellar solution. Different solvents were used in order to prevent aggregation and to completely characterize the side-chain features of both the common and less common aminoacids which compose the macrocyclic ring and the fatty acid side-chain moieties of ST.

The entire study was performed with a batch amount of about 2 mg.

NMR Spectra in D_2O and DMSO

The complete assignment has been obtained using the usual methods used in this kind of 2D NMR study. Particularly the quartet of intensity 1:3:3:1 was

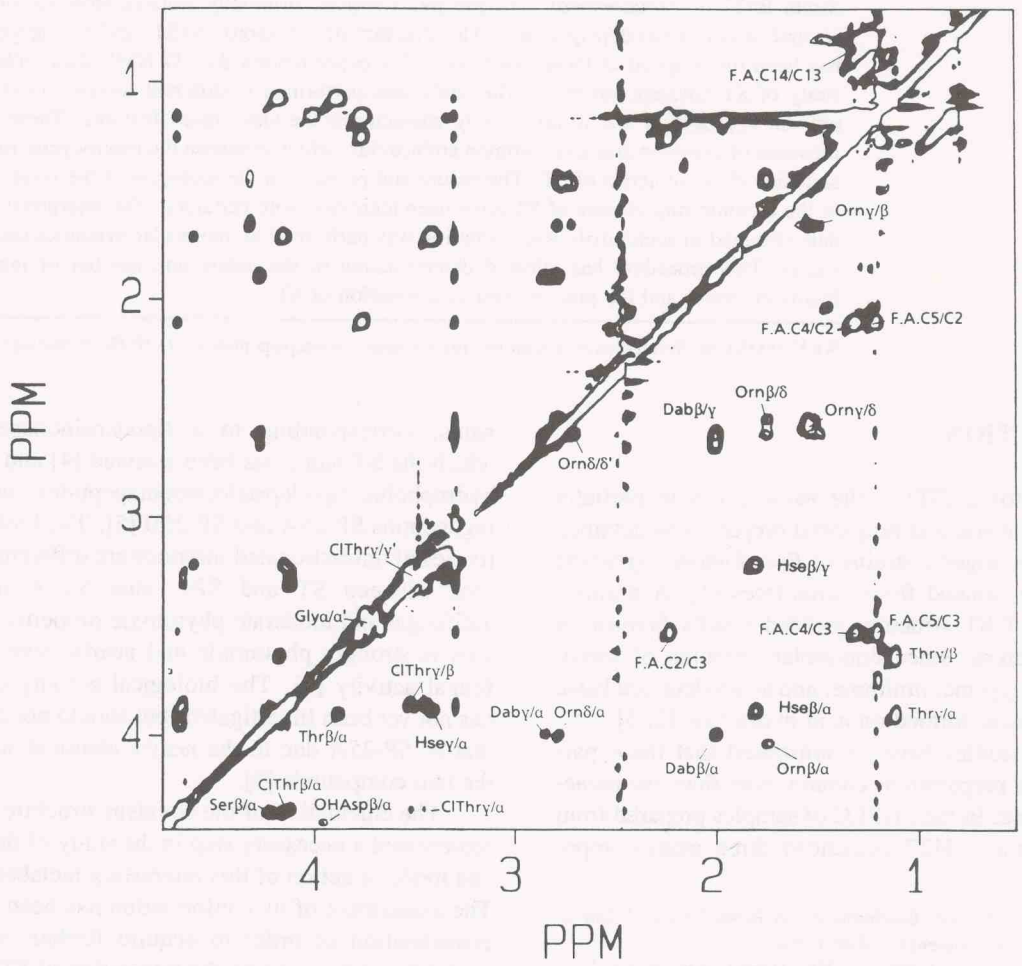

Fig. 1. TOCSY spectrum of ST in DMSO solution. The spectrum was obtained with a mixing time of 180 ms in order to observe the relayed connectivities of the residues side chains. All the spin systems connectivity are clearly visible. As an example the α/β connectivity of the Orn residue which was visible with difficulty in D_2O is clearly discernible. ClThr and OHAsp refer to (4-Cl)Thr and (3-OH)Asp respectively.

straightforwardly assigned to the proton of the CH group of 2,3-dehydro-2-aminobutyric acid moiety (Dhb), which presence was ascertained previously [4].

In the aliphatic region the assignment was performed by identification of the kind and the nature of substituents of the side chains both by the chemical shift indication from literature data [8] and observing the direct and remote scalar connectivities in double quantum filtered correlated spectroscopy (DQF COSY) and total correlated spectroscopy (TOCSY) correlation spectra. All spectra not shown (throughout this paper) are available on request from the authors.

As an example the identification of the Orn side chain was performed by means of the complete assignment.

The connectivities of this long side chain were detected in the TOCSY spectrum as remote connectivities. At this stage the only degenerate spin systems were those due to the two AX systems of Gly and 3-hydroxyaspartic acid (3-OH) Asp and those due to the AM_2X_2 systems of 2,4-diaminobutyric acid (Dab) and HomoSerine (Hse) side chains. The assignment of Gly was performed observing the strong geminal coupling constant ($|J| > 13$ Hz) present in the AB system. The fatty acid (F.A.) side chain, characterized by the presence of the methyl group adjacent to a shielded methylene group, was easily identified.

Also the Dab side chains were both characterized by means of the presence of both direct and remote connectivities. The presence of a methyl group in the spin system in the DQF COSY spectrum led to assign the protons of the side chain of the Thr residue.

Observation of two methylene groups with a terminal one deshielded up to 3.5 ppm led to assign the Hse side chain. Observation of a spin system with two methylene groups with the terminal one deshielded up to 3.5 ppm led to assign the Hse side chain.

Also the spin systems due to (4-Cl) Thr, (3-OH) Asp, and Ser were identified by chemical shifts values and coupling patterns in the TOCSY spectrum.

The DQF COSY in DMSO gave indication about the scalar connectivity between NH and the corresponding CHα protons. TOCSY with a long mixing time allowed the observation of both direct and remote connectivities (see Fig. 1).

In dimethyl sulfoxide (DMSO) solution, the small region bleached in the NMR spectra in D_2O from solvent residual protons was much better observed.

The complete assignments are reported in Table I. The assignments obtained completely agree with those independently reported [7].

Table I. Chemical Shift (ppm) and Related Assignments of NMR Spectra of ST in D_2O, DMSO, and CD_3CN/H_2O

Residue	Assignments	D_2O	DMSO	CD_3CN/H_2O 7:2
Fatty acid	C2	2.43–2.38	2.22	2.01
	C3	3.94	3.89	3.71
	C4	1.47	1.3	1.41
	C5–C13	1.2	1.21	1.23
	C14	0.83	0.83	0.83
Ser	NH	—	8.2	8.38
	Cα	4.85	4.62	4.76
	Cβ	4.65	4.15	4.60–4.26
Dab	NH	—	8.66	8.43
	Cα	4.21	4.38	4.15
	Cβ	2.2	1.97	2.05
	Cγ	3.09	2.80	2.99
Gly	NH	—	8.47	7.95
	Cα	4.07–3.87	3.83–3.63	4.05
Hse	NH	—	8.20	7.50
	Cα	4.37	4.13	4.28
	Cβ	2.1	1.83	2.05–1.90
	Cγ	3.37–3.48	3.51	3.28
Orn	NH	—	8.0	8.83
	Cα	4.45	4.30	4.61
	Cβ	2.0	1.74	1.85
	Cγ	1.68	1.53	1.51
	Cδ	3.0	2.80	2.94
Thr	NH	8.12	8.12	8.18
	Cα	4.15	4.10	4.08
	Cβ	4.10	3.74	4.02
	Cγ	1.36	1.16	1.27
Dhb	NH	—	—	9.31
	Cβ	6.93	6.60	6.82
	Cγ	1.75	1.62	1.63
(3-OH)Asp	NH	—	7.60	7.65
	Cα	5.03	4.72	4.92
	Cβ	4.70	4.06	4.58
(4-Cl)Thr	NH	—	8.13	8.38
	Cα	5.01	4.68	4.86
	Cβ	4.42	4.14	4.34
	Cγ	3.57–3.52	3.56–3.49	3.44

Spectra in Acetonitrile/Water Mixture

The 2D NMR spectra of ST in acetonitrile/water mixture were obtained in order to get information about the chemical structure of ST in a solvent system very similar to water. In fact, the necessity of preventing both chemical exchange of amide protons and aggregation required the use of this kind of mixture as a solvent (see Fig. 2a). The DQF COSY and TOCSY spectra allowed us to obtain the complete assignment particularly of the resonances due to the NH exchangeable protons. The fingerprint region gave the direct connectivities between the resonances of NH and the $C_\alpha H$ protons of the back-

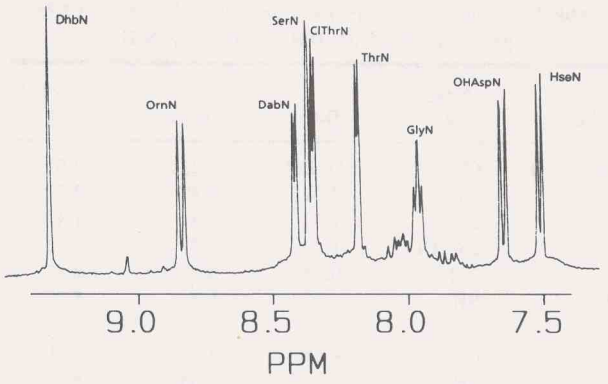

Fig. 2A. 400-MHz NMR spectrum of ST in H_2O/CD_3CN mixture. Spectrum was obtained as reported in the experimental part in a H_2O/CD_3CN mixture 7:2. The spectral region of NH protons 9.5–7.3 ppm is reported. ClThr and OHAsp refer to (4-Cl)Thr and (3-OH)Asp respectively.

bone chain. This DQF COSY spectrum particularly led also to observe the coupling β/β' of Ser and to distinguish it from the spin system of the (3-OH) Asp.

NOE spectrum obtained by a rotating frame dipolar correlated spectroscopy (ROESY) experiment reported in Fig. 2 allowed us to obtain the entire sequential assignment. In fact, the fingerprint region of the spectrum contains the cross peaks due to $NH/C_\alpha H$ dipolar connectivities. Cross peaks between resonances (4-Cl)ThrN/β(3-OH)Asp, DabN/$\beta\beta'$Ser, (3-OH)Asp N/β are also present. The sequential assignments of the sequences (a) Dhb-Thr-Orn-Hse, (b) Ser-Dab-Gly, and (c) (4-Cl)Thr-(3-OH)Asp are reported as a continuous line in the same Fig. 2B. NOE contacts between the resonances due to amide protons were also observed but are not shown. In particular, rather intense NOE cross peaks were observed due to GlyN/NHse, OrnN/NHse, and DhbN/N(3 OH)Asp dipolar connectivities.

The results obtained confirm the primary structure already reported [4, 6, 7].

The complete assignment was also completed by observation of the cross peaks between the NH and both β and γ resonances; these results confirm the assignments and gives a further indication about the through-space proximities. This part of the 2D NMR spectrum, not shown, was completely analyzed. All the NOE cross peaks observed are summarized in Table II, together with an approximate estimate of their relative intensity.

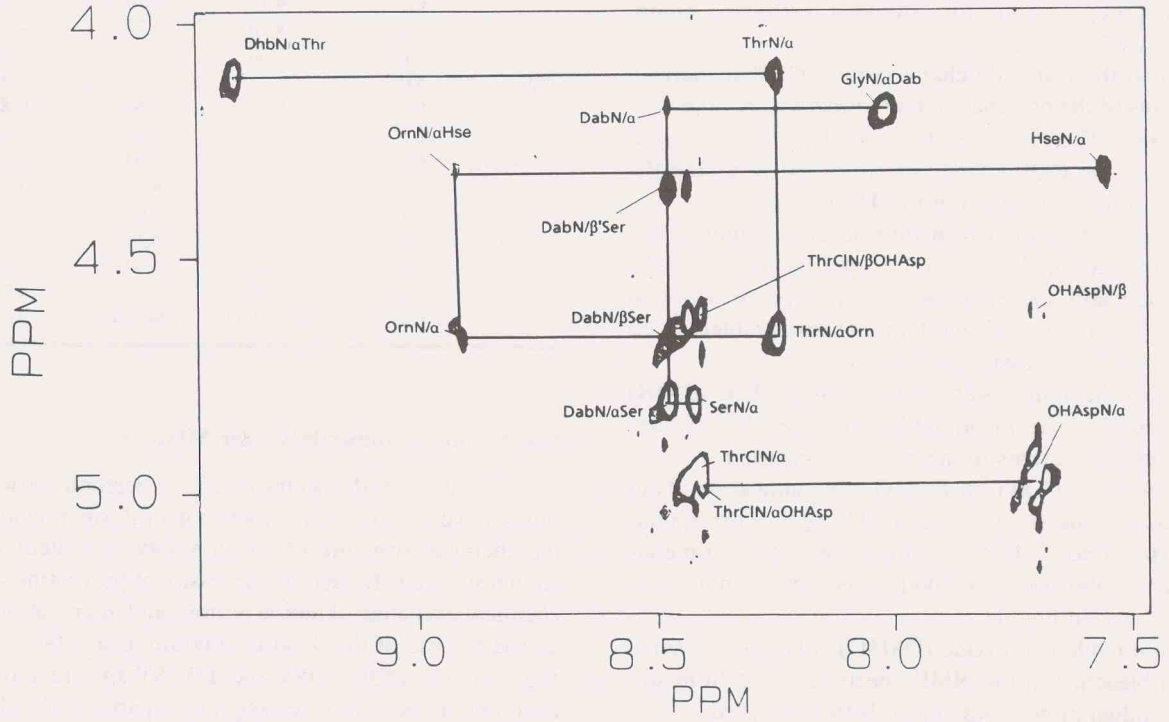

Fig. 2B. ROESY spectrum of ST in H_2O/CD_3CN. NH-CH_α protons region of the ROESY spectrum obtained in H_2O/CD_3CN mixture 7:2 obtained with a mixing time of 100 ms. Solid line indicates sequential connectivities in ST. ClThr and OHAsp refer to (4-Cl)Thr and (3-OH)Asp respectively.

Table II. NOE Effects Observed in the ROESY Spectra of ST[a]

NMR NOE	NMR NOE intensity	Molecular dynamics average over 15 ps (nm)	Molecular dynamics rms fluctuations
C_γH ClThr-C_αH OHAsp	Medium	(v) .53	.03
C_βH ClThr-C_αH Gly	Medium	(v) .54	.05
C_αH Ser-C_αH Dab	Weak	.44	.01
NH Dhb-C_γH aThr	Medium/weak	(v) .41	.04
NH Dhb-C_γH	Medium	(v) .33	.03
NH Orn-C_βH Hse	Weak	(v) .31	.02
NH Orn-C_γH	Medium/strong	(v) .37	.02
NH Orn-C_βH	Medium/weak	.24	.02
NH Orn-C_βH′	Medium/weak	.35	.02
NH Dab-C_γH	Medium/strong	(v) .29	.02
NH Dab-C_βH	Strong	(v) .30	.01
NH Ser-C_αH F.A.	Strong	(v) .25	.02
NH aThr-C_γH	Medium	(v) .43	.01
NH aThr-C_γH Orn	Medium	(v) .43	.03
NH aThr-C_βH Orn	Medium	.42	.02
NH aThr-C_βH′ Orn	Medium	.33	.03
NH Gly-C_βH Dab	Medium/weak	(v) .37	.03
NH Gly-C_γH Dab	Weak	(v) .52	.02
NH Hse-C_γH	Medium/strong	.29	.04
NH Hse-C_γH′	Medium/strong	.35	.02
NH Hse-C_βH	Medium/strong	.34	.01
NH Hse-C_βH′	Medium/strong	.25	.02
NH Dhb-C_αH aThr	Strong	.21	.02
NH aThr-C_αH	Strong	.27	.01
NH aThr-C_αH Orn	Strong	.22	.02
NH Orn-C_αH	Medium/weak	.28	.01
NH Orn-C_αH Hse	Weak	.35	.01
NH Hse-C_αH	Medium	.26	.01
NH OHAsp-C_αH	Medium	.28	.01
NH Ser-C_αH	Medium/strong	.29	.01
NH Dab-C_αH Ser	Strong	.24	.02
NH Dab-C_βH Ser	Medium	.28	.03
NH ClThr-C_βH OHAsp	Medium/weak	.39	.02
NH Dab-C_βH′ Ser	Medium	.41	.02
NH OHAsp-C_βH	Weak	.26	.02
NH DHB-NH OHAsp	Medium/strong	.31	.03
NH Orn-NH Hse	Medium/strong	.30	.03
NH Gly-NH Hse	Medium/strong	.33	.03
NH Orn-NH aThr	Weak	.44	.02
NH Dhb-NH aThr	Medium	.43	.03
NH ClThr-C_βH Dab	Medium	(v) .66	.02
F.A. C2-C4	Medium/strong	(v) .30	.01
NH Gly-C_αH Dab	Strong	.20	.02
NH Dab-C_αH	Weak	.27	.01

[a] The relative intensity is reported as strong, medium, and weak as defined in the experimental part. The internuclear distances (nm) obtained by molecular dynamics simulation are also reported. ClThr and OHAsp refer to (4-Cl)Thr and (3-OH)Asp respectively.
(v): Virtual atom (s). The distance restraint interaction refers to a non-atomic calculated site, center of interaction. Strong, medium, weak distances referred to virtual atoms implicate a correction term (up to 0.1 nm) which must be added to the allowed proton-proton distances.

The residue sequence obtained in the ST molecule was found to be in full agreement with previously reported results [4, 6, 7].

Furthermore, the configuration of all the residues present in ST has been completely determined. Particularly NMR and chromatographic methods gave the complete knowledge of chiralities [4, 6, 7, 9].

Structure of ST in Solution

A molecular dynamics simulation was carried out as reported in the experimental part. The results of the last 15-ps simulation at $T = 300$ K were analyzed in terms of energy, dihedral angles, hydrogen bonds, and NOEs. No large fluctuations in the potential energy were observed, and all the conformations explored during the simulations are energetically permitted. The interproton distances obtained are reported in Table II.

The dihedral angle values obtained for the ring and side chains are available on request to authors.

The occurrences of hydrogen bonds during the molecular dynamics simulation are reported in Table III.

The final backbone conformation and the stereopicture of the whole molecule are reported in Fig. 3 and Fig. 4, respectively. The comparison of the proton-proton distances obtained by NMR and calculations, reported in Table II, shows a general good agreement with the exception of C_γH (4-Cl)Thr-C_αH (3-OH)Asp, C_βH (4-Cl)Thr-C_αH Gly, and NH (4-Cl)Thr-C_βH Dab proton distances that in the molecular dynamics simulation are slightly longer than those suggested by NMR. Since all these cases involve the (4-Cl)Thr residue, it is possible that the (4-Cl)Thr conformation does not represent the

Table III. Hydrogen Bonds Detected during the last 15 ps of Molecular Dynamics (MD) Simulation

HB	Donor-acceptor average distance (nm)	Angle (degrees)	Occurrence (% of time)
NH(Orn)-O(Ser)	.29	159.	92.
NH(Ser)-O(Orn)	.29	161.	91.
NH_2(Orn)-O(Gly)	.31	157.	70.
NH(Hse)-hydroxyl O(Hse)	.29	143.	45.
NH(Gly)-hydroxyl O((4-Cl)Thr)	.33	160.	36.
NH((3-OH)Asp)-O(aThr)	.29	144.	35.
OH(aThr)-O(aThr)	.27	141.	32.
OH(F.A)-O(F.A)	.27	141.	27.
NH(Hse)-O(Dab)	.31	144.	25.

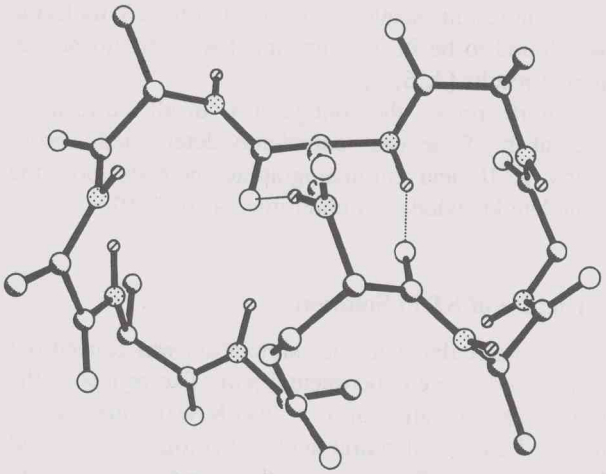

Fig. 3. Backbone conformation of ST (Syringotoxin). The structure was obtained at the end of the equilibration time (15 ps). Dashed lines show hydrogen bonds.

unique possibility for this residue, leading to local flexibility which can give rise to NOE intensity violation.

The results obtained account for the existence of a single conformation for the backbone. Most side-chain torsion angles χ^i, with $i > 1$, indicate a free rotation of side chains. The ring conformation is stabilized by intramolecular hydrogen bonds, as reported in Table III. It has to be noted that, due to the absence of the solvent in the simulation, the occurrence of the hydrogen bonds (column 4 in the table) might not be realistic; in fact the tendency to form intramolecular hydrogen bonds are often overestimated by the calculations. Thus, the backbone conformation appears to be stabilized by only two hydrogen bonds: those involving NH(Orn)—O(Ser) and NH(Ser)—O(Orn) as reported in Fig. 3.

CONCLUSIONS

The complete assignment of 2D NMR spectra of ST in different solvents has been obtained. The solution acetonitrile/water structure of ST was thus determined by 2D NMR NOE data and by in vacuo simulation by molecular dynamics methods. Figure 4 reports the molecular structure obtained together with the side-chain conformation.

It is interesting to note that the overall shape of the molecule resembles approximately that of white line inducing principle (WLIP), a lipodepsipeptide produced by the mushroom saprotroph *Pseudomonas reactans* [10] that contains a β-hydroxydecanoyl group. This shape has been described as the "seam of a tennis ball" and is in agreement with our results.

The backbone conformation of ST is stabilized by two hydrogen bonds, involving NH(Orn)—O(Ser) and NH(Ser)—O(Orn). All CO are external to the tennis ball shape, giving a strong hydrophylic character to the backbone of the molecule. This feature is enhanced by exposure to the solvent of the polar end group of side chains (i.e., Dab and Orn). The fatty acid chain shadows only the hydrophobic pocket of the molecule, which contains the ornithine backbone (the ornithine carbonyl is involved in the hydrogen bond) while the polar end group of the ornithine itself remains well external. Thus, the strongly hydrophobic fatty acid chain is in the appropriate position for protecting both hydrogen bonds from the breaking action of polar solvents. Several NH, CO, and polar ends of side chains appear to be well external, exposed to the solvent, thus giving to the molecular surface shown in Fig. 4 a hydrophilic character which is in full agreement with the high water solubility.

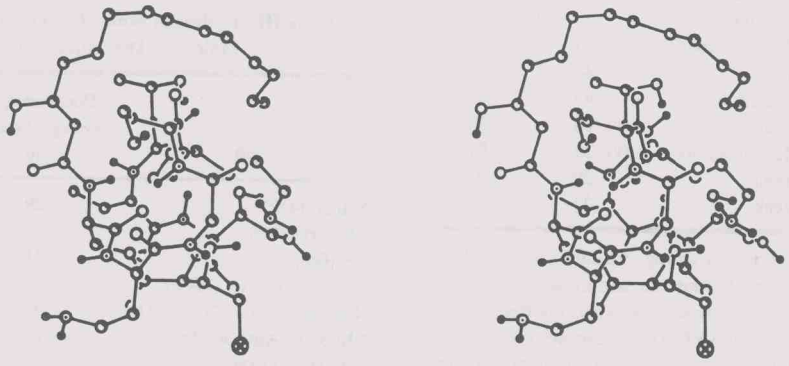

Fig. 4. Stereoview of ST molecule. Conformation of the molecule at the end of the equilibration time (15 ps).

EXPERIMENTAL PROCEDURES

Syringotoxin

Purification and analytical characterization of ST have been previously reported [4].

NMR Spectroscopy

Samples for NMR studies were prepared dissolving about 1 mg of the liophilized sample in 0.5 mL of the following solvents: (a) D_2O; (b) DMSO; (c) CD_3CN/H_2O 7:2 v/v.

NMR spectra of ST (the samples were prepared without any pH correction) were run at 25°C on a Bruker AM 400 instrument operating at 400.13 MHz. The 2D NMR experiments were performed in the phase-time proportional phase increment sensitive mode with (TPPI) phase cycle [11] typically using 2K of memory for 512 increments. The number of scans were optimized in order to obtain a satisfactory signal-to-noise ratio.

Correlation experiments were performed in the double quantum filtered mode (DQF COSY) [12, 13]. Total correlation experiments (TOCSY) were performed using the MLEV-17 spinlock composite pulse sequence [14, 15] with a typical mixing time of 180 ms (relayed) in order to observe remote connectivities.

NOE dipolar correlated 2D spectra were obtained using the NOESY pulse sequence [16] or the rotating frame dipolar correlated 2D spectroscopy ROESY [17, 18]. The mixing time for the magnetization exchange was 100 ms.

Data were processed on a microVax II with the "TRITON" 2D NMR software [19]. Free induction decays (FIDs) were weighted by a sinebell apodization function shifted typically $\pi/3$ in both dimensions.

In all homonuclear 2D experiments, a matrix 1024 × 1024 in the phase-sensitive mode was thus obtained with a digital resolution of about 5 Hz/point. A baseline correction was carried out in both dimensions using a polynomial fit.

Molecular Dynamics Simulation

Molecular dynamics calculations in vacuo were performed with programs from the Groningen molecular simulation system (GROMOS) software package [20–22]. The applied empirical potential energy function contains terms representing covalent bond stretching, bond angle bending, harmonic dihedral angle bending (out-of-plane, out-of-tetrahedral configuration), sinusoidal dihedral torsion, and van der Waals and electrostatic interactions [21]. For the sinusoidal dihedral torsion around $-C_\alpha-CO-$ of the 2,3-dehydro-2-aminobutyric acid (Dhb), which has a partial double-bond character, an energy barrier of 23.0 kJ mol^{-1} was chosen. A dielectric permittivity, $\epsilon = 1$, was used, and the cutoff radius for the nonbonded interactions was chosen in order to include all interactions.

An attractive half-harmonic restraining potential was applied to force the molecule to satisfy selected NOE distances [22]:

$$V_{DR}(d_{kl}) = \tfrac{1}{2}\, k_{DR}(d_{kl} - d^*_{kl})^2 \text{ if } d_{kl} \geq d^*_{kl}$$

$$V_{DR}(d_{kl}) = 0 \qquad \text{if } d_{kl} \leq d^*_{kl}$$

were k_{DR} was 40 kJ mol^{-1} $Å^{-2}$. In order to translate the NOE information into distance ranges d^*_{kl}, we chose an upper limit of 3, 4, and 5 Å for strong, medium, and weak NOEs, respectively, [23]. For the evaluation of this potential all protons were treated explicitly. For all other terms only protons attached to nitrogen or oxygen atoms were treated explicitly.

A bond-stretching term was not included in the calculation; the SHAKE [24] algorithm was used to constrain bond lengths.

The initial conformation of the molecular dynamics simulation was a random one. All atoms were given an initial velocity obtained from a Maxwellian distribution at the desired initial temperature. The rescaling of the temperature during the run was obtained by a coupling with an external path [25] with a time constant t. A time step of 0.002 ps was used in the simulation.

The search of the structure that accounts for the experimental NOEs was performed by the simulated annealing procedure [26], based on a melting of the system followed by a slow cooling.

A first 60-ps simulation at $T = 1000$ K was performed with no inclusion of the restraining potentials that account for the experimental NOEs. To avoid the cis–trans peptide isomerization at this temperature [27], we included a dihedral angle restraining potential in the force field; this is sufficient to maintain the trans conformation in the peptide bond. When the temperature reached 800 K, the dihedral angle restraining potential was switched off and the restraining potentials that take into account the experimental NOEs were included. Finally the system was equilibrated at 300 K for 15 ps.

This procedure gives a conformation in good agreement with experimental NOEs, but with two val-

ues of ϕ angles not compatible with the experimental ^3J coupling constants. In fact ^3J values $CH_\alpha-NH$ relative to Orn and (3-OH)Asp are smaller than those experimentally observed. This anomaly is mostly due to the effect of simulation in vacuo that overestimates the presence of intramolecular hydrogen bonds.

The entire procedure was therefore repeated by restraining the ϕ angles corresponding to ^3J coupling constant values $\geq$ 8 Hz, i.e., ϕ Orn, ϕ Ser, ϕ (4-Cl)Thr, and $\phi \geq$ (3-OH)Asp; thus obtaining a nearly unique acceptable conformation, in good agreement both with NOEs and ^3J values.

ACKNOWLEDGMENTS

This work has been supported in part by grants of the Italian National Research Council (CNR), special ad hoc program "Chimica fine II." A. C. was supported by a fellowship awarded by Italfarmaco SpA, Centro Richerche. Thanks are due to W. F. van Gunsteren for helpful discussions.

REFERENCES

1. Gross, D. C.; DeVay, J. E. *Proc. Am. Phytopathol. Soc.* **1976,** *3*, 269–270.
2. Gross, D. C.; DeVay, J. E.; Stadman, F. H. *J. Appl. Bacteriol.* **1977,** *43*, 453–486.
3. Gonzales, C. F.; DeVay, J. E.; Wakeman, R. *J. Physiol. Mol. Plant Pathol.* **1981,** *18*, 41–50.
4. Ballio, A.; Bossa, F.; Collina, A.; Gallo, M.; Iacobellis, N. S.; Paci, M.; Pucci, P.; Scaloni, A.; Segre, A.; Simmaco, M. *FEBS Lett.* **1990,** *269*, 3777–3780.
5. Ballio, A.; Barra, D.; Bossa, F.; Collina, A.; Grgurina, I., Marino, G.; Moneti, G.; Paci, M.; Pucci, P.; Segre, A. L.; Simmaco, M. *FEBS Lett.* **1991,** *291*, 109–112.
6. Iacobellis, N. S.; Lavermicocca, P.; Grgurina, I.; Simmaco, M.; Ballio, A. *Physiol. Mol. Plant Pathol.* **1992,** *40*, 107–116.
7. Fukuchi, N.; Isogai, A.; Nakayama, J.; Takayama, S.; Yamashita, S.; Suyama, K.; Takemoto, J. Y.; Suzuki, A. *J. Chem. Soc. Perkin Trans. 1* **1992,** 1149–1157.
8. Gross, K.-H.; Kalbitzer, H. R. *J. Magn. Reson.* **1988,** *76*, 87–89.
9. Fukuchi, A.; Isogai, A.; Suzuki, A. *Agric. Biol. Chem.* **1991,** *55*, 625–627.
10. Mortishire-Smith, R. J.; Nutkins, J. C.; Packman, L. C.; Brodey, C. L.; Rainey, P. B.; Johnstone, K.; Williams, D. H. *Tetrahedron* **1991,** *47*, 3645–3654.
11. Marion, D.; Wüthrich, K.; *Biochem. Biophys. Res. Commun.* **1983,** *113*, 967–974.
12. Piantini, U.; Sørensen, O. W.; Ernst, R. R. *J. Am. Chem. Soc.* **1982,** *104*, 6800–6801.
13. Rance, M.; Sørensen, O. W.; Bodenhausen, G.; Wagner, G.; Ernst, R. R.; Wüthrich, K. *Biochem. Biophys. Res. Commun.* **1983,** *117*, 479–485.
14. Braunschweiler, L.; Ernst, R. R. *J. Magn. Reson.* **1983,** *53*, 521–528.
15. Bax, A.; Davis, D. G.; *J. Magn. Reson.* **1985,** *65*, 355–360.
16. Wüthrich, K.; Kogler, G.; Ernst, R. R.; *J. Magn. Res.* **1984,** *58*, 370–388.
17. Bothner-By, A. A.; Stephens, R. L.; Lee, J.; Warren, C. D.; Jeanloz, R. W.; *J. Am. Chem. Soc.* **1984,** *106*, 811–813.
18. Griesinger, C.; Ernst, R. R. *J. Magn. Reson.* **1987,** *75*, 261–271.
19. Boelens, R.; Vuister, G.; *Software for Processing Multidimensional NMR Spectra*; Utrecht: The Netherlands. (Courtesy of Prof. R. Kaptein).
20. Berendsen, H. J. C.; Postma, J. P. M.; van Gunsteren, W. F.; Di Nola, A.; Haak, J. R. *J. Chem. Phys.* **1984,** *81*, 3684–3690.
21. Aqvist, J.; van Gunsteren, W. F.; Leijonmarck, M.; Tapia, O., *J. Mol. Biol.* **1985,** *183*, 461–477.
22. Kaptein, R.; Zuiderweg, E. R. P.; Scheek, R. M.; Boelens, R.; van Gunsteren, W. F. *J. Mol. Biol.* **1985,** *182*, 179–182.
23. Kaptein, R.; Boelens, R.; Scheek, R. M.; van Gunsteren, W. F.; *Biochemistry* **1988,** *27*, 5389–5395.
24. Ryckaert, J. P.; Ciccotti, G.; Berendsen, H. J. C. *Mol. Phys.* **1988,** *34*, 1311–1327.
25. Berendsen, H. J. C.; van Gunsteren, W. F. In *Molecular Liquids. Dynamics and Interactions*, Barnes, A. J., et al. Eds.; NATO ASI Series *C135*, Reidel, Dordrecht, pp. 475–500.
26. Kirkpatrick, S., Gelatt, C. D., Jr. and Vecchi, M. P. *Science* **1983,** *220*, 671–680.
27. Bruccoleri, R. E.; Karplus, M. *Biopolymers* **1990,** *29*, 1847–1862.